International Journal of Heat and Mass Transfer 96 (2016) 406–412

Contents lists available at ScienceDirect

International Journal of Heat and Mass Transfer

journal homepage: www.elsevier.com/locate/ijhmt

Thermal conduction in an orthotropic sphere with circumferentially varying convection heat transfer

D. Sarkar, A. Haji-Sheikh, A. Jain *

Mechanical and Aerospace Engineering Department, University of Texas at Arlington, TX, USA

ARTICLE INFO

Article history:
Received 23 June 2015
Received in revised form 7 January 2016
Accepted 8 January 2016

Keywords:
Convective heat transport
Flow over a sphere
Thermal modeling
Orthotropic heat transfer

ABSTRACT

Heat transfer due to fluid flow past a sphere is encountered commonly in engineering applications. In this case, the local convective heat transfer coefficient on the surface of the sphere is known to change with azimuthal and polar angles due to various flow phenomena. While surface-averaged convective heat transfer coefficient is commonly used for engineering analysis, however, not much work exists for modeling the temperature field inside the sphere while accounting for the spatially varying convective heat transfer, especially in the context of a sphere with orthotropic thermal conduction properties. This paper presents an analytical approach for a steady state solution of this problem by deriving a set of algebraic equations for coefficients of a series solution of the temperature distribution. The problem is solved using two different approaches, which are shown to lead to equivalent results. Temperature distribution based on the analytical approach is found to be in excellent agreement with finite-element simulation results. The effect of various parameters, such as thermal conduction orthotropic ratio, heat generation rate, power density, flow rate, etc. on temperature distribution in the sphere is presented. Results discussed in this paper contribute towards the fundamental understanding of an important heat transfer problem, and in the design of thermal management techniques for engineering applications involving convective cooling of spherical systems.

1. Introduction

Fluid flow past a solid body results in energy exchange between the two through convective heat transfer [1–6]. This process is commonly characterized by the convective heat transfer coefficient, h, which, in general, varies over the fluid–solid interface. While a space-averaged heat transfer coefficient is often adopted as an engineering approximation [4], the effect of the spatial variation of convection on temperature fields is clearly important for a complete understanding of this phenomenon [5]. For the specific case of flow past a sphere, the convective heat transfer coefficient is known to vary with both azimuthal and polar angles, φ and θ, respectively. The dependence of h around the periphery of the sphere has been studied for a variety of flow conditions [1,7]. The heat transfer coefficient h is the largest at the stagnation point ($\varphi = 0°$), following which, h first decreases due to laminar boundary layer development. For laminar flow, a minima is reached at around $\varphi = 109°$ where separation occurs [1]. Similarly, h also varies with θ. The temperature and velocity fields in the flow around the sphere have been measured and numerically computed [8]. The overall heat transfer coefficient has been measured for small spheres in a fluid flow and a relationship between heat transfer, flow velocity and fluid properties has been derived using experimental data [9]. An analytical solution for transient heat transfer from a sphere at low Reynolds number under steady velocity conditions has been developed [10]. Analytical solution for unsteady heat transfer at small Peclet numbers has also been developed when the surface temperature of the sphere undergoes a step change [11].

Most of this past work addresses temperature and velocity fields in the fluid, whereas the temperature field within the sphere, and its dependence on the φ and μ dependent convective heat transfer coefficient has not been adequately addressed in the literature. Such analysis has been carried out in the past for other geometries, including extended surfaces [12–15] and orthotropic cylinders [5], using a variety of analytical techniques to account for the space-dependent convective heat transfer. A Fourier series method has been used to determine the two-dimensional temperature distribution in a rectangular fin with heat transfer coefficient varying along its length [12]. Temperature in fins with varying geometries and heat transfer coefficient has been computed using Frobenius series expansion method [13]. The performance of

* Corresponding author at: 500 W First St, Rm 211, Arlington, TX 76019, USA. Tel.: +1 (817) 272 9338; fax: +1 (817) 272 2952.
E-mail address: jaina@uta.edu (A. Jain).

http://dx.doi.org/10.1016/j.ijheatmasstransfer.2016.01.027
0017-9310/

Nomenclature

h	convective heat transfer coefficient, (W/m^2-K)	R	sphere radius, (m)
k	thermal conductivity, (W/m-K)	T	temperature rise above ambient, (K)
Q	volumetric heat generation rate, (W/m^3)	θ	polar angle
r	radial coordinate, (m)	φ	azimuthal angle
P_n^m	associated Legendre functions of degree n and order m		

annular fins in the presence of variable heat transfer coefficient has been studied [14]. A Galerkin based integral approach has also been adopted to account for variable heat transfer coefficient in fins [15]. An analytical solution for temperature distribution in an orthotropic cylinder with spatially-varying heat transfer coefficient on its surface has been presented [5] by assuming a Fourier series form of the temperature distribution with coefficients that are determined using the spatial variation of the heat transfer coefficient. In addition to such analytical approaches, numerical methods have also been used to analyze cases with space-varying heat transfer coefficient. For example, a finite difference based model has been adopted to study the transient heat transfer of a solid sphere in cross flow [16].

This paper presents an analytical derivation to compute the temperature distribution in a sphere with spatially varying convective heat transfer coefficient on its surface. Thermal conduction within the sphere is assumed to be orthotropic in general, with different thermal conductivity values in r, φ and θ directions. Volumetric heat generation occurs within the sphere, which is cooled on the outside surface with a convective heat transfer coefficient that depends on both azimuthal and polar angles. A Fourier series form of the temperature distribution is assumed. It is shown that the series coefficients can be determined by solving a set of linear algebraic equations that account for the general spatial variation of h on the sphere surface. The temperature distribution computed by this analytical solution is found to be in good agreement with results from finite-element simulations. The dependence of the temperature profile on a number of parameters such as the heat transfer coefficient, thermal conduction orthotropy, etc. is discussed.

The theoretical derivation of temperature field in a sphere with orthotropic thermal properties is important because while most commercial finite-element simulation tools enable analysis of orthotropic thermal conduction in rectangular and cylindrical coordinate systems, the treatment of orthotropic thermal conduction in spherical coordinates is not available. By deriving the temperature distribution for this very general case, the treatment presented here may help expand the capability of thermal analysis in spherical coordinate systems.

2. Analytical model

This section presents the derivation of the steady state temperature distribution in an orthotropic sphere with internal volumetric heat generation and spatially dependent h. Based on the general derivation presented next in Section 2.1, a special case for a partially orthotropic sphere where $k_\varphi = k_\mu$ is presented in Section 2.2. Section 2.3 discusses an alternate analytical approach for solving the general problem. Finally a brief discussion is presented, showing that for isotropic conditions, i.e. all thermal conductivities being the same, the solutions presented for the orthotropic and partially orthotropic cases reduce to that of the isotropic solution as one would expect.

2.1. Orthotropic sphere

Fig. 1 shows a schematic of the general heat transfer problem being addressed in this sub-section. The steady-state governing energy equation in a three dimensional orthotropic sphere is given by [17]

$$k_r\left[\frac{\partial^2 T}{\partial r^2}+\frac{2}{r}\frac{\partial T}{\partial r}\right]+\frac{k_\phi}{r^2(1-\mu^2)}\frac{\partial^2 T}{\partial \varphi^2}+\frac{k_\mu}{r^2}\frac{\partial}{\partial \mu}\left[(1-\mu^2)\frac{\partial T}{\partial \mu}\right]+Q=0 \tag{1}$$

where $T(r,\ \varphi,\ \mu)$ is the temperature rise above ambient, $\mu=\cos(\theta)$, k_r, k_φ and k_μ are thermal conductivities in the r, φ and μ directions, and Q is the volumetric heat generation rate.

The temperature distribution is subject to the following boundary conditions:

$$\frac{\partial T}{\partial r}=0 \quad \text{at } r=0 \tag{2}$$

$$k_r\frac{\partial T}{\partial r}+h(\varphi,\mu)\cdot T=0 \quad \text{at } r=R \tag{3}$$

$$T(r,\varphi,\mu)=T(r,\varphi+2\pi,\mu) \tag{4}$$

$$\left.\frac{\partial T}{\partial \varphi}\right|_{\varphi}=\left.\frac{\partial T}{\partial \varphi}\right|_{\varphi+2\pi} \tag{5}$$

Eq. (2) represents the requirement for the temperature field to be finite at $r=0$. The circumferential variation of h at $r=R$ is accounted for by Eq. (3). Eqs. (4) and (5) represent temperature periodicity and heat flux continuity in the φ-direction. In addition to satisfying Eqs. (1)–(5), the temperature field must also remain bounded in the μ direction [17].

If h were a constant number, then the solution for Eqs. (1)–(5) can be obtained by the separation of variables method in a

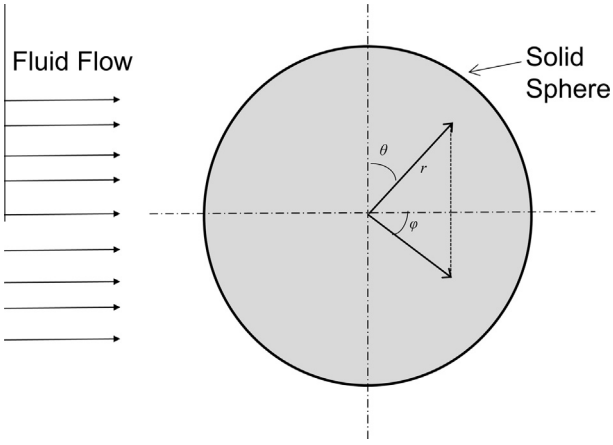

Fig. 1. Schematic of the problem.

straightforward fashion [17]. However, the general case of spatially varying h considered here cannot be addressed by this approach. In this case, the temperature field is first transformed as follows:

$$T(r,\phi,\mu) = w(r,\varphi,\mu) - \frac{Qr^2}{6k_r} \tag{6}$$

In Eq. (6), the second term absorbs the non-homogeneity in the governing equation, thereby leaving a homogeneous governing equation for $w(r, \varphi, \mu)$ and transferring the non-homogeneity to the boundary condition at $r = R$ for w. The set of equations for $w(r, \varphi, \mu)$ is as follows,

$$k_r\left[\frac{\partial^2 w}{\partial r^2}+\frac{2}{r}\frac{\partial w}{\partial r}\right]+\frac{k_\phi}{r^2(1-\mu^2)}\frac{\partial^2 w}{\partial \varphi^2}+\frac{k_\mu}{r^2}\frac{\partial}{\partial \mu}\left[(1-\mu^2)\frac{\partial w}{\partial \mu}\right]=0 \tag{7}$$

subject to

$$\frac{\partial w}{\partial r}=0 \quad \text{at } r=0 \tag{8}$$

$$k_r\frac{\partial w}{\partial r}+h(\varphi,\mu)w=F(\varphi,\mu) \quad \text{at } r=R \tag{9}$$

$$w(r,\varphi,\mu)=w(r,\varphi+2\pi,\mu) \tag{10}$$

$$\left.\frac{\partial w}{\partial \varphi}\right|_{\varphi}=\left.\frac{\partial w}{\partial \varphi}\right|_{\varphi+2\pi} \tag{11}$$

where

$$F(\varphi,\mu)=\frac{QR}{3}\left[1+\frac{h(\varphi,\mu)R}{2k_r}\right] \tag{12}$$

The solution for $w(r, \varphi, \mu)$ is written in the form of the following infinite series:

$$w(r,\phi,\mu)=\sum_{n=0}^{\infty}\sum_{m=0}^{n}C_{nm}\cos(m\varphi)P_n^{\sqrt{\beta}m}(\mu)\left(\frac{r}{R}\right)^{-0.5+\sqrt{\alpha n^2+\alpha n+,0.25}} \tag{13}$$

where $\alpha = k_\mu/k_r$ and $\beta = k_\varphi/k_\mu$.

This particular form of the solution is chosen because it satisfies the governing differential equation (7) and several boundary conditions, given by Eqs. (8), (10) and (11). Note that in general, the associated Legendre functions in Eq. (13) may have non-integer order due to unequal thermal conductivities in the polar and azimuthal directions. The coefficients C_{nm} in Eq. (13) can then be calculated to satisfy the boundary condition at the surface $r = R$, given by Eq. (9). To do so, the form of $w(r, \varphi, \mu)$ given by Eq. (13) is inserted in Eq. (9), resulting in

$$k_r\sum_{n=0}^{\infty}\sum_{m=0}^{n}C_{nm}\cos(m\varphi)P_n^{\sqrt{\beta}m}(\mu)\left(\frac{-0.5+\sqrt{\alpha n^2+\alpha n+0.25}}{R}\right)+h(\varphi,\mu)\sum_{n=0}^{\infty}\sum_{m=0}^{n}C_{nm}\cos(m\varphi)P_n^{\sqrt{\beta}m}(\mu)=F(\varphi,\mu) \tag{14}$$

While Eq. (14) involves infinite series in both polar and azimuthal directions, it can be simplified by multiplying throughout by $\cos(j\varphi)$ and $P_i^{\sqrt{\beta}j}(\mu)$, and then integrating over φ and μ. Since h is in general a function of φ and μ, this results in a set of linear equations involving the unknown coefficients, given by

$$C_{ij}a_{ij}+\sum_{n=0}^{\infty}\sum_{m=0}^{n}C_{nm}b_{ijnm}=f_{ij} \quad \text{for each } i=0,1,2,3,4\ldots \text{ and } j\leqslant i \tag{15}$$

where,

$$a_{ij}=\left(\frac{-0.5+\sqrt{\alpha i^2+\alpha i+0.25}}{R}\right)\int_0^{2\pi}\cos^2(j\varphi)d\varphi\int_{-1}^{1}\left[P_i^{\sqrt{\beta}j}(\mu)\right]^2 d\mu \tag{16}$$

$$b_{ijnm}=\int_0^{2\pi}\int_{-1}^{1}h(\varphi,\mu)P_n^{\sqrt{\beta}m}(\mu)P_i^{\sqrt{\beta}j}(\mu)\cos(m\varphi)\times\cos(j\varphi)d\mu d\varphi \tag{17}$$

$$f_{ij}=\int_0^{2\pi}\int_{-1}^{1}F(\varphi,\mu)P_i^{\sqrt{\beta}j}(\mu)\cos(j\varphi)d\mu d\varphi \tag{18}$$

Assuming that zero through N eigenvalues are considered in the μ-direction, Eq. (15) represents a set of $(N+1)\times(N+2)/2$ linear equations in the same number of unknowns C_{ij}, $i = 0,1,2,\ldots N$ and $j \leqslant i$, from where the unknown coefficients can be computed. For example, if eigenvalues up to $N = 10$ are considered, the total number of unknown coefficients is 66. Once the coefficients are computed, Eqs. (6) and (13) represent the temperature distribution in the orthotropic cylinder. Note that in the special case of h being a constant, the integral in the expression for b_{ijmn} in Eq. (17) would yield all zero values except when $i = n$ and $j = m$ due to orthogonality of the eigenfunctions [17]. As a result, for this case, the coefficients C_{ij} can be computed explicitly, given by $(a_{ij} + d_{ijij})\ C_{ij} = f_{ij}$. This special case is the commonly used separation of variables approach where all coefficients are determined explicitly in case h is a constant. For the more general case of spatially varying h considered here, a set of linear algebraic equations given by Eqs. (15)–(18) are to be solved to determine the series coefficients.

The next sub-section considers two special cases in which the fully orthotropic thermal conduction within the cylinder is relaxed.

2.2. Partially orthotropic and isotropic sphere

In several engineering applications, thermal conduction in the sphere may be partially orthotropic. For example, when the sphere is made up of multiple concentric layers, thermal conductivity in the radial direction may be lower than the other two components due to thermal contact resistance between layers, whereas thermal conductivities in the azimuthal and polar directions may be equal, $k_\varphi = k_\mu = k_c$, where k_c is a constant. The temperature distribution in such a case may be obtained from the treatment in Section 2.1 by setting $k_\varphi = k_\mu = k_c$, and hence $\beta = 1$. The temperature distribution is still given by Eq. (6), but the modified form for $w(r, \varphi, \mu)$ is as follows

$$w(r,\phi,\mu)=\sum_{n=0}^{\infty}\sum_{m=0}^{n}C_{nm}\cos(m\varphi)P_n^{m}(\mu)\left(\frac{r}{R}\right)^{-0.5+\sqrt{\alpha n^2+\alpha n+0.25}} \tag{19}$$

In this case, the eigenfunctions in the μ direction are associated Legendre polynomials, a special case of associated Legendre functions that appear in Eq. (13), with integer order, since $\beta = 1$.

The procedure to determine the unknown coefficients C_{nm} in Eq. (19) remains the same as before. The matrix elements a_{ij}, b_{ijnm} and f_{ij} are somewhat simplified, and are now given by,

$$a_{ij}=\left(\frac{-0.5+\sqrt{\alpha i^2+\alpha i+0.25}}{R}\right)\int_0^{2\pi}\cos^2(j\varphi)d\varphi\int_{-1}^{1}\left[P_i^{j}(\mu)\right]^2 d\mu \tag{20}$$

$$b_{ijnm}=\int_0^{2\pi}\int_{-1}^{1}h(\varphi,\mu)P_n^{m}(\mu)P_i^{j}(\mu)\cos(m\phi)\cos(j\varphi)d\mu d\varphi \tag{21}$$

$$f_{ij}=\int_0^{2\pi}\int_{-1}^{1}F(\varphi,\mu)P_i^{j}(\mu)\cos(j\varphi)d\mu d\varphi \tag{22}$$

Note that the integer order of the associated Legendre polynomials leads to significant reduction in computational cost. Explicit expressions for the integrals in Eqs. (20)–(22) are available for integer order only [17–19]. These integrals can also be computed symbolically [20] for any arbitrary, even function $h(\varphi, \mu)$. In comparison, for the more general, orthotropic case discussed in

Section 2.1, exact expressions for the norm integral, as well as the double integrals for b_{ijnm} and f_{ij} are not available, and must be computed numerically.

As a further step, substituting $k_r = k_c$ in equations above reduces the temperature distribution to the special case of an isotropic sphere with identical thermal conductivity in all directions. In this case, while $T(r, \varphi, \mu)$ is still given by Eq. (6), $w(r, \varphi, \mu)$ has a simplified form given by

$$w(r,\phi,\mu) = \sum_{n=0}^{\infty}\sum_{m=0}^{n} C_{nm}\cos(m\varphi)P_n^m(\mu)\left(\frac{r}{R}\right)^n \tag{23}$$

The coefficients are still governed by a set of linear algebraic equations given by Eq. (15). b_{ijmn} and f_{ij} are given by Eqs. (21) and (22) respectively. Due to isotropy in thermal conductivity, expression for a_{ij} given previously by Eq. (20) can be simplified further to

$$a_{ij} = \left(\frac{i}{R}\right)\int_0^{2\pi}\cos^2(j\varphi)d\varphi\int_{-1}^{1}\left[P_i^j(\mu)\right]^2 d\mu \tag{24}$$

2.3. Alternate analytical approach for orthotropic sphere

This section presents an alternate approach for solving the general problem involving orthotropic thermal conduction given by Eqs. (1)–(5) in Section 2.1. In this approach, the temperature is still transformed as given by Eq. (6). However, instead of Eq. (13), the functional form for $w(r, \varphi, \mu)$ is written as follows

$$w(r,\phi,\mu) = \sum_{n=0}^{\infty}\sum_{m=0}^{n} C_{nm}\cos(m\varphi)P_{\eta_n}^{\nu_m}(\mu)\left(\frac{r}{R}\right)^n \tag{25}$$

where $\eta_n = -0.5 + \sqrt{\overline{\alpha}n^2 + \overline{\alpha}n + 0.25}$, $\overline{\alpha} = 1/\alpha$, and $\nu_m = \beta m$. α and β are ratios of thermal conductivities as defined earlier in Section 2.1. In general, η_n and ν_m, the degree and order respectively of the associated Legendre function in Eq. (25) can be non-integers [21]. Due to the arbitrary nature of both degree and order, the associated Legendre function appearing in Eq. (25) is now expressed by a Gauss hypergeometric series [17,21]. Such functions are encountered, for example in problems related to a sphere surface cut by a cone [17].

Note that similar to Eq. (13), the functional form of w represented by Eq. (25) satisfies Eqs. (7), (8), (10) and (11), and the series coefficients C_{nm} may be determined using a procedure similar to Section 2.1 utilizing the boundary condition involving the spatially varying convective heat transfer coefficient, given by Eq. (9).

$$k_r\sum_{n=0}^{\infty}\sum_{m=0}^{n} C_{nm}\cos(m\varphi)P_{\eta_n}^{\nu_m}(\mu)\left(\frac{n}{R}\right) + h(\varphi,\mu)\sum_{n=0}^{\infty}\sum_{m=0}^{n} C_{nm}\cos(m\varphi)P_{\eta_n}^{\nu_m}(\mu) = F(\varphi,\mu) \tag{26}$$

Similar to Section 2.1, Eq. (26) is multiplied throughout by $\cos(j\varphi)$ and $P_{\eta_i}^{\nu_j}(\mu)$ to result in the following linear system for the series coefficients

$$C_{ij}a_{ij} + \sum_{n=0}^{\infty}\sum_{m=0}^{n} C_{mn}b_{ijnm} = f_{ij} \quad \text{for each } i = 0,1,2,3,4\ldots n \text{ and } j \leqslant i \tag{27}$$

where

$$a_{ij} = \left(\frac{i}{R}\right)\int_0^{2\pi}\cos^2(j\varphi)d\varphi\int_{-1}^{1}\left[P_{\eta_i}^{\nu_j}(\mu)\right]^2 d\mu \tag{28}$$

$$b_{ijnm} = \int_0^{2\pi}\int_{-1}^{1} h(\varphi,\mu)P_{\eta_n}^{\nu_m}(\mu)P_{\eta_i}^{\nu_j}(\mu)\cos(m\varphi)\cos(j\varphi)d\mu d\varphi \tag{29}$$

$$f_{ij} = \int_0^{2\pi}\int_{-1}^{1} F(\varphi,\mu)P_{\eta_i}^{\nu_j}(\mu)\cos(j\varphi)d\mu d\varphi \tag{30}$$

In general, the associated Legendre function is defined by the Gauss hypergeometric series in the region $|\mu^2| < 1$ for any arbitrary μ, η and ν [21]. Substituting $\alpha = \beta = 1$ in Eq. (25) results in the solution for isotropic thermal conduction within the sphere, as expected.

Thus, a general solution for temperature in an orthotropic spherical body has been derived in two different ways, and special, less restrictive cases have been discussed. In the next section, the various theoretical models presented in this section are computed. Results are compared against finite element simulations, and the effect of various properties and geometry on the temperature distribution is discussed.

3. Results and discussion

Fig. 2 shows a polar plot of temperature distribution in a solid sphere of radius 10 cm with uniform heat generation rate, $Q = 1432.39\ \text{W/m}^3$, based on a total heat generation rate of 6 W in the sphere. The φ variation of h is chosen to be $h(\varphi) = h_0(1 + \cos^2(\varphi/2))$ with $h_0 = 100\ \text{W/m}^2\ \text{K}$, an even function with maxima at $\varphi = 0$ and $\varphi = \pi$, and minima at $\varphi = \pi/2$. Radial, azimuthal and polar thermal conductivities are assumed to be $k_r = 0.2$ W/m-K, $k_\mu = 20$ W/m-K and $k_\varphi = 30$ W/m-K respectively, consistent with the expectation that for a sphere made of multiple layered materials, the radial thermal conductivity will be the lowest due to multiple thermal contact resistances between layers. Temperature variation in Fig. 2 is predominantly in the radial direction due to the low value of k_r relative to k_μ and k_φ. The temperature gradient in the φ direction is seen more clearly in Fig. 3, which presents line plots of temperature distribution for the isotropic sphere ($k = 0.2$ W/m-K) as a function of r along the plane $\theta = \pi/2$ and $\varphi = 0$ which is the region that includes the stagnation point (Fig. 3(a)), and similarly temperature as a function of φ at $r = R$ (Fig. 3(b)). Inset in Fig. 3(b) shows the variation of h as a function of φ. The location of the maxima in temperature coincides with the minima in h, which is also along expected lines. Fig. 3 (a) and(b) also present comparison of the temperature distribution obtained from the analytical model discussed in Section 2 for the isotropic case with results from finite-element simulation. The

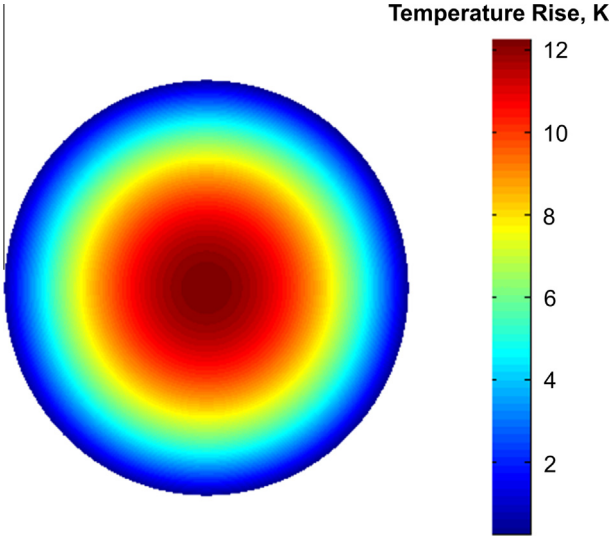

Fig. 2. Polar plot for temperature distribution for an orthotropic sphere with $k_r = 0.2$ W/m-K, $k_\varphi = 30$ W/m-K and $k_\mu = 20$ W/m-K.

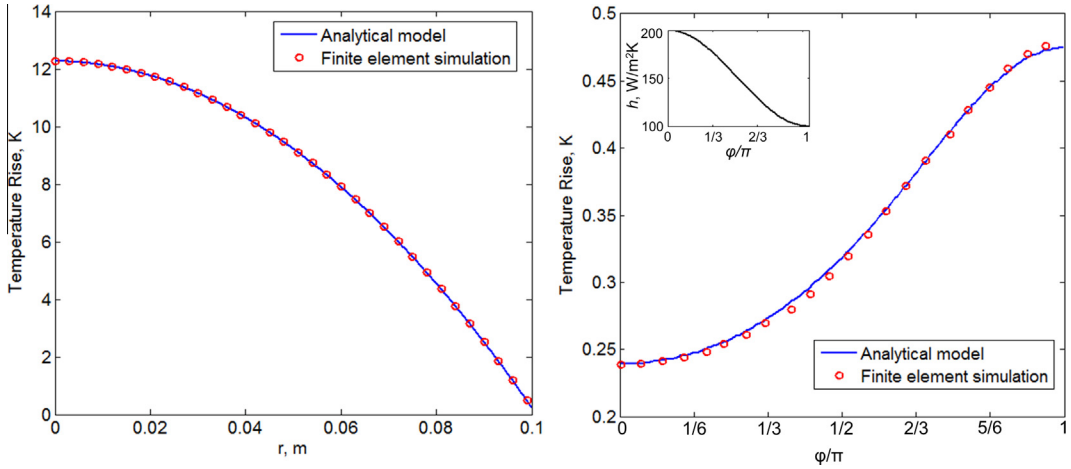

Fig. 3. Comparison of analytical solution for the temperature distribution in an isotropic sphere with finite element simulations: (a) variation with r (b) variation with φ.

finite-element simulations are carried out in ANSYS CFX, with sufficiently refined grid to rule out grid dependence. Good agreement is found between the temperature distribution computed from Eqs. (6), (23) and (24) and the one predicted by the finite element model. Note that since orthotropic thermal conduction in spherical coordinate systems cannot be modeled in ANSYS CFX, the comparison between analytical model and finite-element simulations shown in Fig. 3 has been carried out only for the case of isotropic thermal conduction.

Fig. 4 shows temperature variation in the radial direction with changing values of k_r, while holding k_φ and k_μ at a constant value of 0.2 W/m-K. The temperature increases as k_r reduces, as expected. It is found that the partially orthotropic temperature distribution given by Eq. (19) reduces to the temperature solution for an isotropic sphere given by Eq. (24), also shown in Fig. 4. Fig. 5 analyzes a different case, where k_r is held constant at 0.2 W/m-K, and k_φ is varied. The value of k_μ is held equal to k_φ. Fig. 5 plots the temperature as a function of φ along the surface at $r = R$ and $\mu = 0$. As expected, the peak temperature of the temperature curves illustrated in Fig. 5 reduce as k_φ increases. The inset in Fig. 5 shows the variation of h with φ. As expected, the maxima in temperature coincides with minima in the heat transfer coefficient.

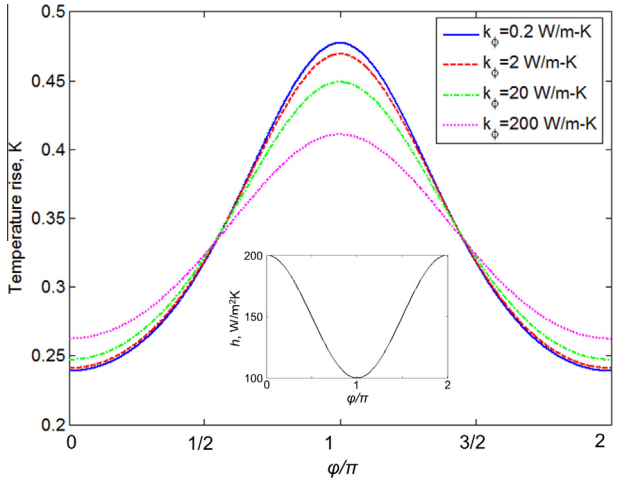

Fig. 5. Plot for temperature distribution in an orthotropic sphere as a function of φ for different values of k_φ while maintaining $k_r = 0.2$ W/m-K. The value of k_μ is equal to the k_φ for each case.

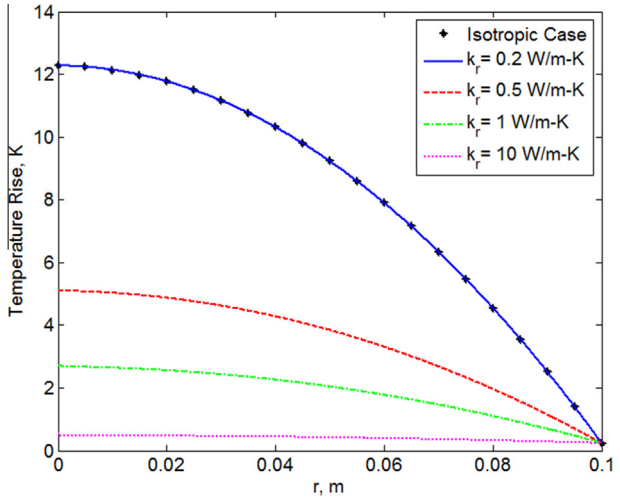

Fig. 4. Plot for temperature distribution in an orthotropic sphere versus as a function of r for different values of k_r while maintaining $k_\varphi = k_\mu = 0.2$ W/m-K.

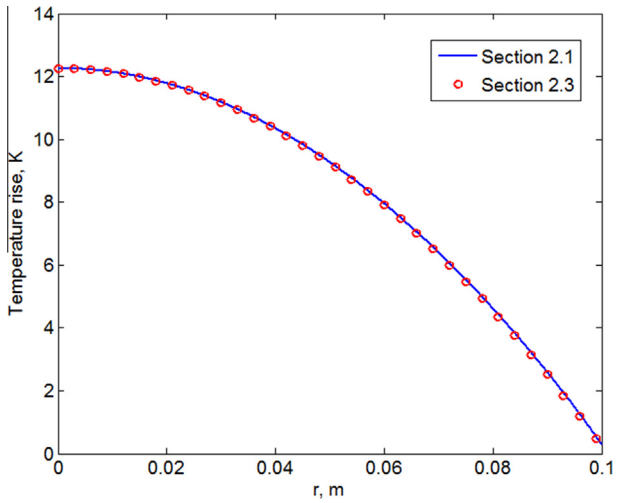

Fig. 6. Plot for temperature distribution in an orthotropic sphere as a function of radius using two different solution techniques, for $k_r = 0.2$ W/m-K, $k_\varphi = 30$ W/m-K and $k_\mu = 20$ W/m-K.

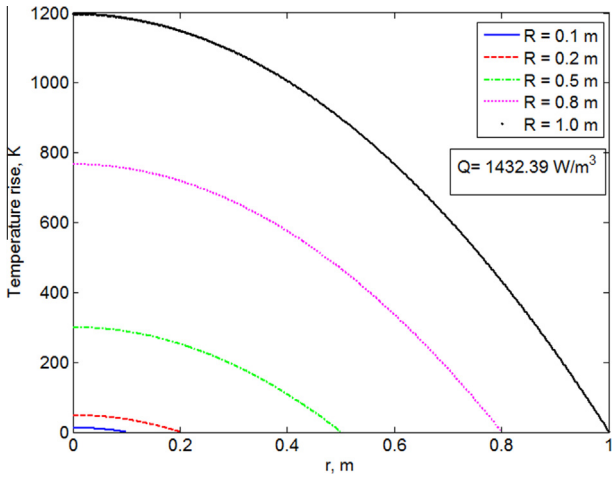

Fig. 7. Plot for temperature distribution in an orthotropic sphere as a function of r for spheres of different radii R, while maintaining constant internal heat generation rate.

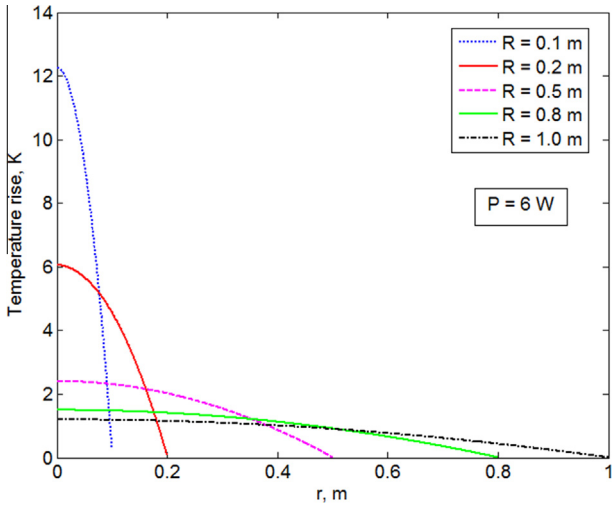

Fig. 8. Plot for temperature distribution in an orthotropic sphere versus r for spheres of different radii R, while maintaining constant power.

Fig. 6 shows a comparison of the temperature distribution as a function of r for the two solution techniques discussed in Sections 2.1 and 2.3. There is good agreement between the two solutions, as expected, which shows that either of the two approaches discussed in Sections 2.1 and 2.3 may be adopted for computing temperature field in a general, orthotropic sphere.

Fig. 7 illustrates the variation in radial temperature distribution in spheres of different sizes with the volumetric heat generation rate maintained constant. The value of the volumetric heat generation rate is based on 6 W power in a solid sphere of radius 0.1 m as the reference case. As expected, a sphere with a larger radius has a larger temperature gradient, due to greater power generated inside the sphere of a larger radius. Conversely, in Fig. 8, the total power is held constant at 6 W, and it is found that there is greater temperature rise in the small radius sphere due to the increased volumetric heat generation rate.

Finally, Fig. 9 analyses the temperature variation in the radial and azimuthal directions as functions of convective cooling rates. As expected, the peak temperature drops in both cases with increase in the cooling rate. The reduction in temperature is less significant at higher values of h_0, which could be because at high h_0, total thermal resistance is dominated by thermal conduction within the sphere rather than convective thermal resistance at the boundary.

4. Conclusions

This paper addresses the classical problem of heat transfer between a solid sphere and fluid flow past its surface. The analytical technique presented here accounts for spatial variation of the heat transfer coefficient on the sphere surface, as well as orthotropic thermal conduction within the sphere. The temperature field inside the sphere is expressed in a series form, where the coefficients are determined by solving a set of linear algebraic equations. Results derived from two different approaches agree well with each other. The results presented in this manuscript contribute towards the understanding of a classical heat transfer problem, and enables the analysis of an orthotropic sphere which is not possible in current finite-element analysis tools. This paper may contribute towards the development of design tools for thermal management of heat-generating spherical systems with realistic convective heat transfer coefficients.

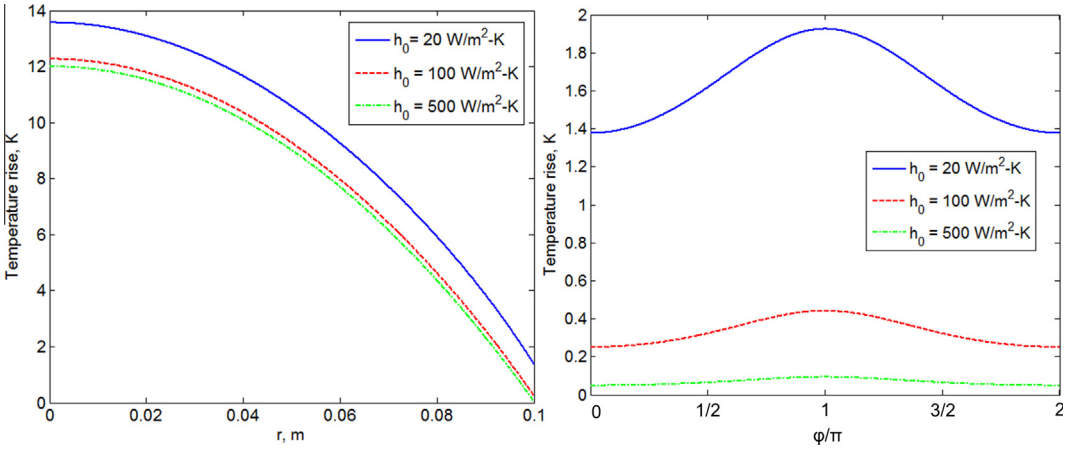

Fig. 9. Plot for temperature distribution in an orthotropic sphere for different convective cooling rates h_0: (a) variation with r, (b) variation with φ.

References

[1] H. Schilichting, Boundary Layer Theory, Pergamon Press Ltd., 1955.
[2] T. Yuge, Experiments on heat transfer of spheres including combined natural and forced convection, J. Heat Transfer 82 (3) (1960) 214–220.
[3] A. Zukauskas, J. Ziugzda, Heat Transfer of a Cylinder in Crossflow, Hemisphere Publishing Corp, Washington, DC, 1985. 219 p. Translation. 1.
[4] T.L. Bergman, A.S. Lavine, F.P. Incropera, D.P. DeWitt, Fundamentals of Heat and Mass Transfer, John Wiley & Sons, 2011.
[5] D. Sarkar, K. Shah, A. Haji-Sheikh, A. Jain, Analytical modeling of temperature distribution in an anisotropic cylinder with circumferentially-varying convective heat transfer, Int. J. Heat Mass Transfer 79 (2014) 1027–1033.
[6] D.Q. Kern, A.D. Kraus, Extended surface heat transfer, McGraw-Hill, 1972.
[7] J.I. Shell, Die Wärmeübergangszahl von Kugelflächen, Bull. Acad. Sci. Nat. Belgrade 189 (4) (1938).
[8] T.A. Johnson, V.C. Patel, Flow past a sphere up to a Reynolds number of 300, J. Fluid Mech. 378 (1999) 19–70.
[9] H. Kramers, Heat transfer from spheres to flowing media, Physica 12 (2–3) (1946) 61–80.
[10] P.N. Choudhoury, D.G. Drake, Unsteady heat transfer from a sphere in a low Reynolds number flow, Q. J. Mech. Appl. Math. 24 (1971) 23–36.
[11] Z.G. Feng, E.E. Michaelides, Unsteady heat transfer from a sphere at small Peclet numbers, J. Fluids Eng. 118 (1) (1996) 96–102.
[12] S.W. Ma, A.I. Behbahani, Y.G. Tsuei, Two-dimensional rectangular fin with variable heat transfer coefficient, Int. J. Heat Mass Transfer 34 (1) (1991) 79–85.
[13] B. Kundu, P.K. Das, Performance analysis and optimization of straight taper fins with variable heat transfer coefficient, Int. J. Heat Mass Transfer 45 (24) (2002) 4739–4751.
[14] E. Mokheimer, Performance of annular fins with different profiles subject to variable heat transfer coefficient, Int. J. Heat Mass Transfer 45 (17) (2002) 3631–3642.
[15] A.G. Agwu Nnanna, A. Haji-Sheikh, D. Agonafer, Effect of variable heat transfer coefficient, fin geometry, and curvature on the thermal performance of extended surfaces, J. Electron. Packaging 125 (3) (2003) 456–460.
[16] B. Abramzon, C. Elata, Unsteady heat transfer from a single sphere in Stokes flow, Int. J. Heat Mass Transfer 27 (5) (1984) 687–695.
[17] N.M. Ozisik, Heat Conduction, John Wiley & Sons, 1980.
[18] N.N. Lebedev, Richard R. Silverman, Special Functions and Their Applications, Prentice Hall Inc., 1965.
[19] W. Bell, Special functions for scientists and engineers, D. Von Nostrand Company Ltd., 1968.
[20] S. Wolfram, The MATHEMATICA Book, 4th ed., Cambridge University Press, Wolfram Research Inc., 1999.
[21] Milton. Abramowitz, Irene A. Stegun, Handbook of Mathematical Functions with Formulas, Graphs, and Mathematical Tables, Dover Publications, New York, 1972.